# Tunable Donor−Acceptor Interactions in 4-Ene/Yne-Ferrocenyl and 4-Enamine Naphthalimides with Ferrocenyl Headgroups

C. John McAdam,*,† Joy L. Morgan,† Brian H. Robinson,*,† Jim Simpson,† Philip H. Rieger,‡ and Anne L. Rieger‡

*Department of Chemistry, University of Otago, Dunedin, New Zealand, and Department of Chemistry, Brown University, Providence, Rhode Island*

*Received June 17, 2003*

A series of 4-(X)-substituted naphthalimides (X = ethenylFc, ethynylFc, piperidinyl, ethenylpiperidinyl, ethenylpyrrolidinyl) with ferrocenyl headgroups (R = $Fc(CH_2)_n$, $n$ = 1, 5, 11) and analogous ethenylFc, ethynylFc, and ethynylFc# (Fc# = octamethylferrocenyl) compounds with a methyl headgroup have been investigated. These are the first 4-enamine-1,8-naphthalimides to be reported. Spectrochemical properties for all compounds are presented and the X-ray structures of 4-piperidinyl and 4-ethynylferrocenyl derivatives described. This series of donor−acceptor derivatives allows a correlation between the degree of internal charge separation, UV−vis and emission properties, and mediation by the organometallic redox couple. Charge separation increases in the order 4-amino ≪ 4-C=C-amino ≅ 4-C≡CFc ≅ 4-C=CFc < 4-C≡CFc#. The unsaturated spacer is the key influence on both $\lambda_{flu}$ and $\phi_f$, but $\lambda_{flu}$ is independent of the headgroup due to the imide node. In contrast, $\phi_f$ shows a "distance" effect for the ferrocenyl headgroup, and as a result $\phi_f$ can be "tuned"; dyads with the $Fc(CH_2)_{11}$ headgroup have $\phi_f > 0.2$. Solvatochromism data gives an excited state dipole of ∼8 D. An EPR study of radical anions provides a description of the SOMO. Through-space interaction between the ferrocenyl headgroup and the charge-separated excited state may account for some of the trends in EPR and $\phi_f$. In general, emission is decreased upon oxidation to the ferrocenium analogues.



## Introduction

A wide variety of electron donor−acceptor arrays have been designed to mimic bacterial photosynthetic charge separation, incorporate photoinduced electron transfer, and provide new materials for electroluminescent and nonlinear optical applications[1]. 1,8-Naphthalimides are good candidates as components of donor−acceptor arrays because as good acceptors they often exhibit strong solvatochromatic,[2,3] hydrogen-bonding,[4] and cation-dependent[5,6] fluorescence. Emission is accentuated if there is a 4-amino substituent, and quantum yields of 0.7−0.8 are routinely encountered for 4-amino-*N*-alkylnaphthalimides.[2,3,6,7] These features have been exploited in biological fluorescent labeling,[8] optical brighteners,[9] pH-dependent sensors,[10] laser[11] and electroluminscent[12] dyes, liquid crystals,[13] and CT-initiated multistep dark

* Corresponding author. Fax: +64 3 479 7906. E-mail: mcadamj@alkali.otago.ac.nz.
† University of Otago.
‡ Brown University.

(1) (a) Sauvage, J.-P.; Collin, J.-P.; Chambron, J.-C.; Guillerez, S.; Coudret, C.; Balzani, V.; Barigelletti, F.; de Cola, L.; Flamigni, L. *Chem. Rev.* **1994**, *94*, 993. (b) Gust, D.; Moore, T. A.; Moore, A. L. *Acc. Chem. Res.* **1993**, *26*, 198. (c) Wasielewski, M. R.; Gaines, G. L.; O'Neil, M. P., Niemczyk, M. P., Svec, W. A., Eds. *Supramolecular Arrays;* Kluwer: Dordrecht, 1992. (d) Ashwell, G. J., Bloor, D., Eds. *Organic Materials for Nonlinear Optics III*; Royal Society of Chemistry: Cambridge, 1993; p 219. (e) Lehn, J. M. *Supramolecular Chemistry*; VCH: Weinheim, 1995. (f) Balzani, V., Candola, F., Eds. *Supramolecular Photochemistry*; Horwood: Chichester, England, 1991. (g) Desvergne J.-P., Czarnik, A. W., Eds. *Chemosensors of Ion and Molecule Recognition*; Kluwer: Dordrecht, 1997.

(2) (a) Alexiou, M. S.; Tychopoulos, V.; Ghorbanian, S.; Tyman, J. H. P.; Brown, R. G.; Brittain, P. I. *J. Chem. Soc., Perkin Trans. 2* **1990**, 837. (b) Yuan, D.; Brown, R. G. *J. Phys. Chem., A* **1997**, *101*, 3461.

(3) Pardo, A.; Poyato, J. M. L.; Martin, E.; Camacho, J. J.; Reyman, D.; Brana, M. F.; Castellano, J. M. *J. Photochem. Photobiol. A* **1989**, *46*, 323.

(4) (a) Niemz, A.; Rotello, V. M. *J. Am. Chem. Soc.* **1997**, *119*, 6833. (b) Deans, R.; Niemz, A.; Breinlinger, E. C.; Rotello, V. M. *J. Am. Chem. Soc.* **1997**, *119*, 10863.

(5) (a) Poteau, X.; Brown, A. I.; Brown, R. G.; Holmes, C.; Matthew, D. *Dyes Pigm.* **2000**, *47*, 91. (b) Mitchell, K.; Brown, R. G.; Yuan, D.; Chang, S.-C.; Utecht, R. E.; Lewis, D. E. *J. Photochem. Photobiol. A: Chem.* **1998**, *115*, 157.

(6) (a) De Silva, A. P.; Gunaratne, H. Q. N.; Gunnlaugsson, T.; Huxley, A. J. M.; McCoy, C. P.; Rademacher, J. T.; Rice, T. E. *Chem. Rev.* **1997**, *97*, 1515. (b) De Silva, A. P.; Gunaratne, H. Q. N.; Gunnlaugsson, T.; McCoy, C. P.; Maxwell, P. R. S.; Rademacher, J. T.; Rice, T. E. *Pure Appl. Chem.* **1996**, *68*, 1443.

(7) (a) Karamancheva, I.; Tadjer, A.; Philipova, T.; Madjarova, G.; Ivanova, C.; Grozeva, T. *Dyes Pigm.* **1998**, *36*, 273. (b) Korol'kova, N. V.; Val'kova, G. A.; Shigorin, D. N.; Shigalevskii, V. A.; Vostrova, V. N. *Russ. J. Phys. Chem.* **1990**, *64*, 393. (c) Philipova, T. *J Prakt. Chem./Chem.-Ztg.* **1994**, *336*, 587. (d) Grabtchev, I.; Philipova, T.; Meallier, P.; Guittonneau, S. *Dyes Pigm.* **1996**, *31*, 31.

(8) (a) Stewart, W. W. *Nature* **1981**, *292*, 17. (b) Hodgkiss, R. J.; Jones, G. W.; Long, A.; Middleton, R. W.; Parrick, J.; Stratford, M. R. L.; Wardman, P.; Wilson, G. D. *J Med. Chem.* **1991**, *34*, 2268. (c) Liu, Z.-R.; Hecker, K. H.; Rill, R. L. *J. Biomol. Struct. Dyn.* **1996**, *14*, 331.

(9) (a) Peters, A. T.; Bide, M. J. *Dyes Pigm.* **1985**, *6* 349. (b) Konstantinova, T. N.; Meallier, P.; Grabtchev, I. *Dyes Pigm.* **1993**, *22*, 191.

(10) (a) Yuan, D.; Brown, R. G. *J. Chem. Res.*, (*S*) **1994**, 418. (b) De Silva, A. P.; Gunaratne, H. Q. N.; Habib-Jiwan, J.-L.; McCoy, C. P.; Rice, T. E.; Soumillion, J.-P. *Angew. Chem., Int. Ed. Engl.* **1995**, *34*, 1728. (c) Czarnik, A. W. *Acc. Chem. Res.* **1994**, *27*, 302; (d) Bissell, R. A.; De Silva, A. P.; Gunaratne, H. Q. N.; Lynch, P. L. M.; Macguire, G. E. M.; McCoy, C. P.; Sandanayake, K. R. A. S. *Top. Curr. Chem.* **1993**, *168*, 223.

10.1021/om0304659 CCC: $25.00 
Publication on Web 10/28/2003

electron transfers in linear triads.[14] Recently, we reported[15] the preparation and electrochemical properties of naphthalimide (**1**) and 4-halonaphthalimide (**2**) derivatives with *N*-ferrocenyl headgroups and showed that the ferrocenyl headgroup did not perturb the ground or excited state because of the node at the carboxamide terminus. Tian and co-workers[16] have also investigated a variety of ferrocenyl derivatives linked to the naphthalimide by *N*-isoquinoline or 4-amino-CH=N or saturated spacers and investigated applications in electroluminescent devices.[17] They found that the inhibition of photoinduced electron transfer (PET) pathways is dependent on the spacer and oxidation state of the ferrocenyl group.

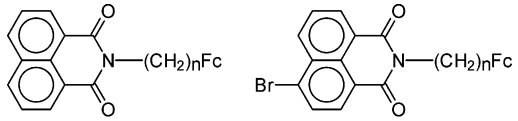


**1** **2**

Compounds **1** and **2** reported in our previous paper do not have the donor−acceptor capacity to participate in the internal charge separation in the excited states which leads to the good quantum yields exhibited by 4-amino-*N*-alkyl-1,8-naphthalimides. An interest in fluorescent organometallic arrays led us to prepare dyads of the type shown in Figure 1 and to consider two aspects of internal charge separation in ferrocenyl arrays. The first is whether CT characteristics are modified in 4-amino derivatives with *N*-alkylferrocenyl headgroups as the carboxamide node should negate any influence of the ferrocenyl (or ferrocenium) headgroup; furthermore, there may well be a distance effect[18] depending on the length of the *N*-alkyl chain. The second aspect is whether the interpolation of an unsaturated link to the aromatic fluorophore would accentuate the charge separation. Polarization of the $\pi$ system of the derivatives of the general configuration shown was expected to lead to a strong donor−acceptor interaction (Figure 1), which would change the excited state characteristics from the usual $\pi\pi^*$ to a lowest excited singlet state, primarily CT in nature; the orientation may facilitate subsequent electron transfer reactions by an electric field effect. An additional point was whether the charge separation could be mediated by having a redox-active 4-ferrocenyl substituent. This arises because oxidation of the ferrocenyl group associated with the unsaturated spacer converts the 4-substituent into an acceptor with consequential reversal of the polarity of the CT excited state to a $Fc^+$←(organic fluorophore),[19] a configuration that has been established in dyads where C=CFc and −C≡CFc groups are linked to aromatic fluorophores.[20]

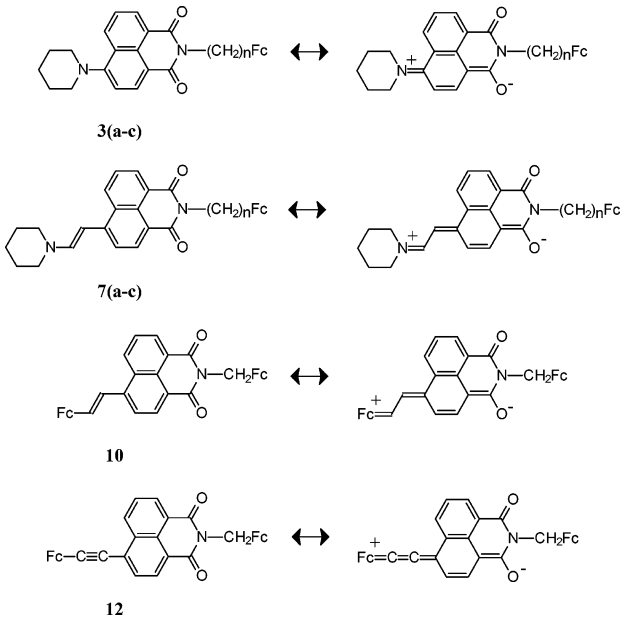


**Figure 1.** Selected naphthalimides and examples of their charge transfer state.

Herein, we present a spectroscopic and spectroelectrochemical investigation of 4-substituted naphthalimides with *N*-alkylferrocenyl headgroups of the configuration shown in Figure 1 and their oxidized counterparts; related molecules with *N*-methyl headgroups are included for comparison. Compounds **7a**−**c** and **8** represent the first reported 4-aminoethenylnaphthalimides.

## Results and Discussion

Precursors 4-bromo-*N*-(alkylferrocenyl)-1,8-naphthalimides, **2a**−**c** [**a** = $CH_2Fc$, **b** = $(CH_2)_5Fc$, **c** = $(CH_2)_{11}$-Fc], were synthesized directly from 4-bromo-1,8-naphthalic anhydride as previously described.[15] Direct reaction between **2a**−**c** and piperidine solvent at elevated temperatures gave the yellow-orange 4-piperidinyl-*N*-(alkylferrocenyl)-1,8-naphthalimides **3a**−**c** in quantitative yields (Scheme 1). The analogue of **3** with a methyl headgroup, **4**, is known.[21] **3a**−**c** were soluble in $CH_2Cl_2$ and aromatic solvents, moderately soluble in MeCN, and poorly soluble in MeOH.

The synthetic strategy for the preparation of the 4-(*E*)-ethenylpiperidinyl **7a**−**c** and 4-(*E*)-ethenylpyrrolidinyl

(11) Pardo, A.; Martin, E.; Poyato, J. M. L.; Camacho, J. J.; Guerra, J. M.; Weigand, R.; Brana, M. F.; Castellano, J. M. *J. Photochem. Photobiol. A: Chem.* **1989**, *48*, 259.
(12) (a) Morgado, J.; Gruner, J.; Walcott, S. P.; Yong, T. M.; Cervini, R.; Moratti, S. C.; Holmes, A. B.; Friend, R. H. *Synth. Met.* **1998**, *95*, 113. (b) Cacialli, F.; Bouche, C.-M.; Le Barny, P.; Friend, R. H.; Facoetti, H.; Soyer, F.; Robin, P. *Opt. Mater.* **1998**, *9*, 163.
(13) Martynski, T.; Mykowska, E.; Bauman, D. *J. Mol. Struct.* **1994**, *325*, 161.
(14) (a) Greenfield, S. R.; Svec, W. A.; Gosztola, D. J.; Wasielewski, M. R. *J. Am. Chem. Soc.* **1996**, *118*, 6767. (b) Wiederrecht, G. P.; Yoon, B. A.; Svec, W. A.; Wasielewski, M. R. *J. Am. Chem. Soc.* **1997**, *119*, 3358.
(15) McAdam, C. J.; Robinson, B. H.; Simpson, J. *Organometallics* **2000**, *19*, 3644.
(16) (a) Wang, Z.; Chen, K.; Tian, H. *Chem. Lett.* **1999**, *5*, 423. (b) Tian, H.; Xu, T.; Zhao, Y.; Chen, K. *J. Chem. Soc., Perkin Trans. 2* **1999**, 545.
(17) (a) Tian, H.; Su, J.; Chen, K.; Wong, T. C.; Gao, Z. Q.; Lee, C. S.; Lee, S. T. *Opt. Mater.* **2000**, *14*, 91. (b) Gan, J.; Tian, H.; Wang, Z.; Chen, K.; Hill, J.; Lane, P. A.; Rahn, M. D.; Fox, A. M.; Bradley, D. D. C. *J. Organomet. Chem.* **2002**, *645*, 168.
(18) De Silva, A. P.; Gunartne, H. Q. N.; Lynch, P. L. M.; Patty, A. J.; Spence, G. L. *J. Chem. Soc., Perkin Trans. 2* **1993**, *9*, 1611.
(19) (a) Barlow, S.; Marder, S. R. *J. Chem. Soc., Chem. Commun.* **2000**, 1555. (b) Toma, S.; Gaplovsky, A.; Hudecek, M.; Langfelderova, Z. *Monatsch. Chem.* **1985**, *116*, 357. (c) Mendiratta, A.; Barlow, S.; Day, M. W.; Marder, S. R. *Organometallics* **1999**, *18*, 454.
(20) Flood, A.; McAdam, C. J.; Gordon, K. C.; Hudson, R. D.; Manning, A. R.; Robinson, B. H.; Simpson, J. Manuscript in preparation.
(21) (a) Knyazhanskii, M. I.; Metelitsa, A. V.; Alekseev, Y. E.; Pyshchev, A. I.; Kovaleva, T. V.; Sudareva, T. P.; Uzhinov, B. M. *Russ. J. Org. Chem.* **2000**, *36*, 1192. (b) Alekseev, Y. E.; Knyazhanskii, M. I.; Metelitsa, A. V.; Sudareva, T. P.; Zhdanov, Y. A. *Dokl. Akad. Nauk.* **2000**, *370*, 190.

**Scheme 1**[a]

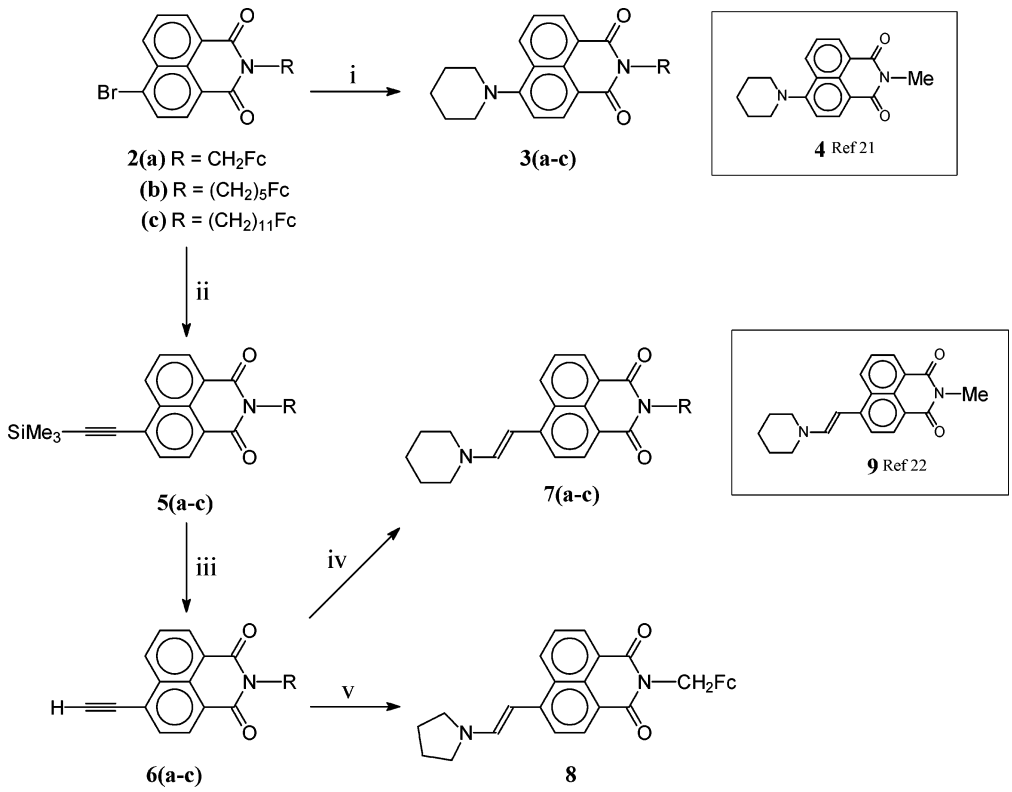


[a] (i) Piperidine, reflux; (ii) trimethylsilylacetylene, $PdCl_2(PPh_3)_2$, CuI, $^iPr_2NH$, reflux; (iii) $K_2CO_3$, MeOH, 20 °C; (iv) piperidine, 20 °C; (v) pyrrolidine, 20 °C.

**8** enamines is also shown in Scheme 1. Surprisingly, these are the first reported ethenylnaphthalimides; the archetypal 4-(*E*)-ethenylpiperidinyl-*N*-methyl-1,8-naphthalimide **9** is described elsewhere.[22] Trimethylsilylacetylene reacted with **2a**−**c** under standard Sonogashira coupling conditions to give the 4-ethynyltrimethylsilyl-*N*-alkylferrocenyl-1,8-naphthalimides **5a**−**c**. Desilylation of **5a**−**c** with $K_2CO_3$/MeOH gave the terminal alkynes **6a**−**c**, which then underwent facile 1,2-conjugate addition of piperidine to give the 4-(*E*)-ethenylpiperidinyl-*N*-alkylferrocenyl-1,8-naphthalimides **7a**−**c**. Similarly reaction of pyrrolidine with **6a** gave 4-(*E*)-ethenylpyrrolidinyl-*N*-methylferrocenyl-1,8-naphthalimide, **8**.

Michael-type additions have been documented for electron-deficient alkynes,[23] allowing nucleophilic attack at the terminal alkynyl carbon. Amination of alkynes is also a well-established process for the preparation of aminoethenyl compounds.[24] However, most alkynes, even *p*-nitrophenyl acetylene,[24b] react only at elevated temperatures or high pressures. While the strong electron-withdrawing effect of the naphthalimide backbone will assist the addition reaction in our compounds, charge separation (Figure 1) allowing delocalization of the electron density to the naphthalimide LUMO would be another driver for facile nucleophilic attack at the alkyne terminus.

**Scheme 2**[a]

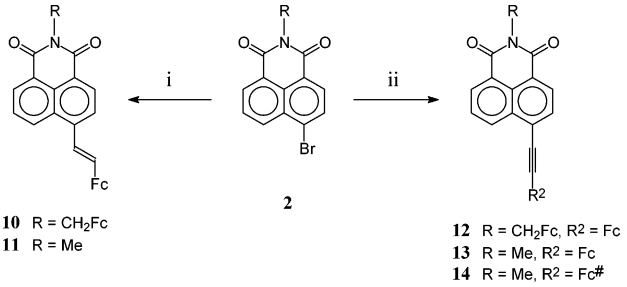


[a] (i) Fc-CH═$CH_2$, $Pd(OAc)_2$, DMF, P(*o*-tolyl)$_3$, $NEt_3$, 80 °C; (ii) $R^2$-$C_2$-H, $PdCl_2(PPh_3)_2$, CuI, $^iPr_2NH$, reflux.

Introduction of the 4-ferrocenyl redox center with a −C═C− spacer to give **10** was achieved by the reaction of ethenylferrocene with **2a** under standard Heck coupling conditions (Scheme 2). The *N*-methyl analogue **11** was prepared by the same route. All the ethenyl compounds had a characteristic intense red color. The sterically preferred *E* configuration for the ethenylnaphthalimides was unambiguously established from $^1$H and 2D NMR techniques. Typical AB coupling constants ($J$ = 16 Hz) were seen for the ferrocenyl compounds **10** and **11**, while those for **7a**−**c** and **8** (13 Hz) are characteristic of arylenamines.[24c] For **7a**−**c** and **8** $\nu$(C═O) are shifted to lower energy than the 4-substituted saturated analogues, attributed to strong coupling with $\nu$(C═C). The ethynyl compounds **5a**−**c** and **6a**−**c** have $\nu$(C≡C) at 2150 and 2100 cm$^{-1}$, respectively, typical of trimethylsilyl and terminal alkynes.

Rapid degradation of the enamines **7**−**9** was observed in acid and base or during chromatography on silica gel. The susceptibility of enamines to hydrolysis is well

(22) McAdam, C. J.; Murray, E.; Morgan, J. L.; Robinson, B. H.; Simpson, J. Novel Naphthalimides and Methods for their Preparation. Provisional patent NZ 523165, Dec 2002.

(23) Jung, M. In *Comprehensive Organic Synthesis*; Trost, B., Fleming, I., Eds.; Pergamon: Oxford, U.K., 1991; Vol. 4, p 41.

(24) (a) Chekulaeva, I.; Kondrat'eva, L. *Russ. Chem. Rev.* **1965**, *34*, 669. (b) Papanastassiou, Z.; Bruni, R.; White, E. *J. Med. Chem.* **1967**, *10*, 701. (c) Müller, T. J. J.; Robert, J. P.; Schmalzlin, E.; Brauchle, C.; Meerholz, K. *Org. Lett.* **2000**, *2*, 2419.

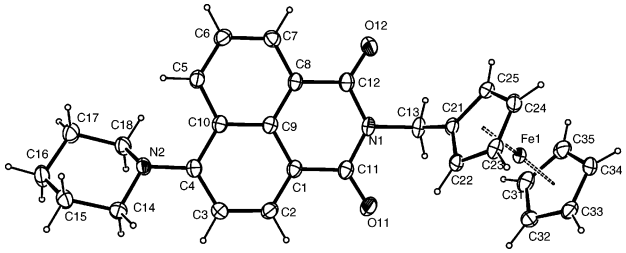


**Figure 2.** Perspective view (ORTEP3)[26] of **3a** showing the atom-numbering scheme, with displacement ellipsoids drawn at the 50% probability level. For clarity, only two C atoms of consecutively numbered cyclopentadienyl rings have been labeled.

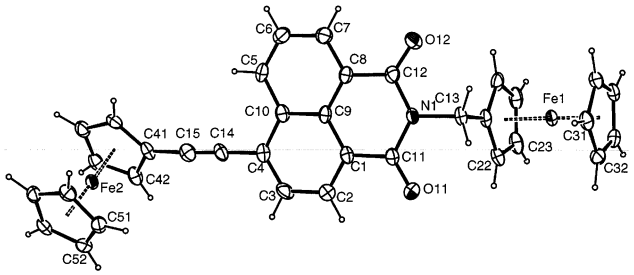


**Figure 3.** Perspective view (ORTEP3)[26] of **12** showing the atom-numbering scheme, with displacement ellipsoids drawn at the 50% probability level. For clarity, only two C atoms of consecutively numbered cyclopentadienyl rings have been labeled.

documented[25] where the rate-determining step in basic media is the attack of water$^-$ on the immonium ion (SI Scheme 3). A combination of the strong naphthalimide acceptor stabilizing the carbinolamine and the basicity of piperidine encourage the hydrolysis reaction for **7**.

The 4-ferrocenyl compound with a −C≡C− spacer, **12**, was prepared from **2a** by Sonogashira coupling with ethynylferrocene (Scheme 2); similar reactions of ethynylferrocene and ethynyloctamethylferrocene with 4-bromo-*N*-methylnaphthalimide gave **13** and **14** with a methyl headgroup. Like their ethenyl analogues, the ethynylferrocene compounds are an intense dark red color. This contrasts with **5** and **6**, which despite the presence of an unsaturated spacer are pale yellow. This clearly indicates the participation of the ferrocene in excited state processes. $\nu$(C≡C) for **12** and **13** at 2200 cm$^{-1}$ are typical of ferrocenylalkynes;[20] $\nu$(C≡C) at 2188 cm$^{-1}$ for **14**, which is an intense dark green color, reflects the influence of the electron-donating methyl substituents on the Cp ring.

Compounds **3**−**14** were stable in dry air and were fully characterized by elemental analysis, ES MS, and complete $^1$H NMR assignment. The ethenylamine compounds **7a**−**c** and **8** contained varying amounts of water in the lattice. The X-ray structures of two derivatives **3a** and **12** were determined and are sufficiently similar to be discussed together. Perspective views of **3a** and **12** are shown in Figures 2 and 3, respectively; these figures define the atom-numbering schemes used for the structural and NMR data. Selected bond length and angle data for both molecules appear in Table 1. Each structure has a ferrocenyl headgroup linked to the naphthalimide through a methylene group. In **3a**, a piperidine substituent is bound at C4 through the piperidine N atom, while for **12** the naphthalimide carries an ethynylferrocene substituent linked through the alkyne C14 atom in the 4-position.

**Table 1. Selected Bond Lengths (Å) and Angles (deg) for 3a and 12**

| | 3a | 12 |
|---|---|---|
| C(1)−C(2) | 1.369(2) | 1.373(3) |
| C(1)−C(9) | 1.419(2) | 1.417(3) |
| C(1)−C(11) | 1.473(2) | 1.492(3) |
| C(2)−C(3) | 1.406(2) | 1.416(3) |
| C(3)−C(4) | 1.389(2) | 1.371(3) |
| C(4)−N(2) | 1.4088(19) | |
| N(2)−C(14) | 1.460(2) | |
| N(2)−C(18) | 1.484(2) | |
| C(14)−C(15) | 1.528(2) | |
| C(15)−C(16) | 1.529(2) | |
| C(16)−C(17) | 1.522(2) | |
| C(17)−C(18) | 1.523(2) | |
| C(4)−C(14) | | 1.478(3) |
| C(14)−C(15) | | 1.160(3) |
| C(15)−C(41) | | 1.447(3) |
| C(4)−C(10) | 1.434(2) | 1.430(3) |
| C(5)−C(6) | 1.369(2) | 1.355(3) |
| C(5)−C(10) | 1.418(2) | 1.421(3) |
| C(6)−C(7) | 1.399(2) | 1.404(3) |
| C(7)−C(8) | 1.382(2) | 1.385(3) |
| C(8)−C(9) | 1.406(2) | 1.409(3) |
| C(8)−C(12) | 1.480(2) | 1.479(3) |
| C(9)−C(10) | 1.423(2) | 1.431(3) |
| C(11)−O(11) | 1.2252(19) | 1.207(3) |
| C(11)−N(1) | 1.396(2) | 1.399(3) |
| C(12)−O(12) | 1.2123(19) | 1.218(3) |
| C(12)−N(1) | 1.404(2) | 1.405(3) |
| N(1)−C(13) | 1.4785(18) | 1.491(3) |
| C(13)−C(21) | 1.506(2) | 1.506(3) |
| C(21)···C(25) ring av C−C | 1.424(3) | 1.424(7) |
| C(31)···C(35) ring av C−C | 1.418(5) | 1.423(8) |
| C(41)···C(45) ring av C−C | | 1.431(13) |
| C(41)···C(45) ring av C−C | | 1.424(3) |
| Fe(1)−C(21−25) av | 2.050(7) | 2.044(2) |
| Fe(1)−C(31−35) av | 2.051(8) | 2.045(10) |
| Fe(1)−C(41−45) av | | 2.047(13) |
| Fe(1)−C(51−55) av | | 2.052(8) |
| O(11)−C(11)−N(1) | 119.91(14) | 120.6(2) |
| O(11)−C(11)−C(1) | 123.44(15) | 122.6(2) |
| N(1)−C(11)−C(1) | 116.65(13) | 116.77(19) |
| C(11)−N(1)−C(12) | 125.17(12) | 124.68(18) |
| C(11)−N(1)−C(13) | 116.93(12) | 117.39(18) |
| C(12)−N(1)−C(13) | 117.88(13) | 117.45(18) |
| O(12)−C(12)−N(1) | 120.22(14) | 119.7(2) |
| O(12)−C(12)−C(8) | 122.90(14) | 123.4(2) |
| N(1)−C(12)−C(8) | 116.87(13) | 116.95(19) |
| N(1)−C(13)−C(21) | 112.50(12) | 109.06(18) |
| C(3)−C(4)−N(2) | 123.36(14) | |
| C(10)−C(4)−N(2) | 117.71(13) | |
| C(3)−C(4)−C(14) | | 120.6(2) |
| C(10)−C(4)−C(14) | | 119.6(2) |
| C(4)−C(14)−C(15) | | 177.0(2) |
| C(14)−C(15)−C(41) | | 176.6(2) |

The naphthalimide skeletons are essentially coplanar in both molecules (maximum deviations C4, 0.1138(13) Å for **3a** and C12, 0.0928(18) Å for **12**). The methylene carbon atoms, C13, bound to the ferrocenyl rings lie within 0.095(2) Å for **3a** and 0.204(3) Å of the naphthalimide ring plane for **12**. For **3a** the N2 atom of the piperidine ring lies 0.2682(17) Å from the naphthalimide ring plane in the same direction as C13, whereas in **12** the C14 atom is located 0.075(3) Å out of the naphthalimide ring plane again on the same side as C13. In both molecules the methyl ferrocenyl moieties are oriented such that the N1−C13−C21 planes are approximately perpendicular to the dicarboximide planes (interplanar

(25) Sollenberger, P. Y.; Martin, R. B. *J. Am. Chem. Soc.* **1970**, *92*, 4261−70.

angles 87.8(1)° for **3** and 89.7(1)° for **12**). The cyclopentadiene rings of the ferrocenylmethyl moiety of **3a** are inclined at 68.48(4)° (C21···C25) and 66.31(4)° (C31···C35) to the naphthalimide ring plane, an orientation similar to that observed previously in 3-nitro-(*N*-ferrocenylmethyl)-1,8-naphthalimide.[15] The cyclopentadiene rings are approximately eclipsed with an angle of 3.39(11)° between the cyclopentadiene ring planes and a mean Fe1−ring distance of 1.656(1) Å. In contrast, for **12** the approximately eclipsed cyclopentadiene rings of the methylene-bound ferrocene moiety lie approximately orthogonal to the naphthalimide ring plane, 82.65(7)° (C21···C25) and 83.15(7)° (C31···C35). The angle between the cyclopentadiene ring planes is 1.87(18)° with a mean Fe1−ring distance of 1.647(1) Å.

Bond lengths and angles in the naphthalenedicarboximide systems for **3a** and **12** compare well with those found in similar systems. In particular, bond length variations within the dicarboximide ring are consistent with extensive electron delocalization over the naphthalimide unit. This does not however extend to the ferrocenyl methyl substituents as noted previously.[27] For **12** there is little evidence for delocalization between the naphthalimide and ferrocenyl moieties in the alkyne ferrocene substituent. The C14≡C15 bond (1.160(3) Å) is short and the C4−C14 (1.478(3) Å) and C14−C41 (1.447(3) Å) vectors are long in comparison to those found in related systems.[28] The approximately eclipsed cyclopentadiene rings of the substituent have an interplanar angle of 2.9(1)° and a mean Fe2−ring distance of 1.650(1) Å. The substituted cyclopentadiene ring of the alkyne ferrocene moiety subtends an angle of 35.51(7)° to the naphthalimide ring plane, and the ferrocenyl moieties bound to the methylene and alkyne residues respectively are oriented to lie on opposite faces of the naphthalimide, which may aid packing of the molecular unit, vide infra. Some delocalization from the N2 lone pair of the piperidine to the naphthalimide ring is indicated for **3a** by the short N2−C4 distance of 1.4088(19) Å. The ring adopts a classic chair conformation with bond lengths and angles closely comparable to those observed in other systems with piperidine N-bound to a polyaromatic ring system.[29] Again, the ferrocenylmethyl and piperidine substituents lie on opposite sides of the naphthalimide ring plane.

The solid state structures of **3a** and **12** are stabilized by weak offset $\pi$-stacking interactions involving the rings of the naphthalenedicarboximide moieties. Both molecules stack in a head-to-tail fashion facilitated by the relative placement of the substituents on the headgroups and at the 4-positions on opposite sides of the naphthalimide ring planes. For **3a** the stacking interactions extend parallel to the *BC* plane, while, for **12**, stacking is restricted to pairs of adjacent molecules. For **3a** the perpendicular distances between the offset rings are in the range 3.32−3.45 Å, with interplanar angles 0.02−4.45° and displacement angles between the rings of 37−43°.[30] The corresponding values for the stacked pairs for **12** are as follows: inter-ring distances 3.31−3.44 Å, interplanar angles 0.00−2.75°, and displacement angles in the range 19−40°.

**Electrochemistry. 3a−c**, **5−7a−c**, and **8** with no 4-ferrocenyl substituent display a one-electron chemically reversible [$Fc^+$/Fc] couple. Potentials for the [$Fc^+$/Fc] couple fall into two sets. First, those with a $FcCH_2$ headgroup have potentials in the range 0.59 ± 0.1 V, slightly anodic of $E_{1/2}$ = 0.55 V for ferrocene, as expected for a naphthalimide group acting as an electron-withdrawing substituent. Second, isolation of the ferrocenyl headgroup from the naphthalimide by the long alkyl chain with a $Fc(CH_2)_n$ ($n$ = 5, 11) headgroup shifts $[Fc]^{+/0}$ cathodically to 0.49 ± 0.1 V.[15] $[Fc]^{+/0}$ for 4-ethenylferrocene **11** and 4-ethynylferrocene **13** without a ferrocenyl headgroup is 0.60 and 0.72 V, respectively; predictably this shifts cathodically to 0.30 V for the 4-ethynyloctamethylferrocene derivative **14**. Because the carboximide node effectively truncates any charge transfer from the ferrocenyl headgroup to the 4-substituent in the ground state, $[Fc]^{+/0}$ for molecules with the 4-ferrocenyl substituent linked to the naphthalimide by an unsaturated spacer **10** and **12** are summative (Table 2). The $[C{\equiv}CFc]^{+/0}$ substituent potential is 0.71 V,[20] and hence two $[Fc]^{+/0}$ at 0.58 and 0.71 V are observed for **12**. For **10** the headgroup and substituent ferrocenyl potentials are similar {$[C{=}CFc]^{+/0} \approx 0.61$ V}, resulting in an apparent two-electron voltammetric wave at 0.60 V.

**Electronic and Emission Spectra of Neutral and Oxidized Compounds.** Selected UV−vis data are given in Table 2; Figure 4 shows $\lambda_{abs}$ spectra for **3a**, **7a**, and **10**. $\lambda_{abs}$ bands below 360 nm ($\epsilon$ > 25 000) are $\pi\pi^*$ transitions (SI Table 2b). Of significance for 4-amine derivatives are the lowest energy transitions at $\lambda_{abs}$ 360−450 nm ($\epsilon$ > 5000), the charge transfer character of which has been examined by a number of workers.[3,5−7,31] These are designated as band A in Table 2 and arise through charge separation in the singlet excited state. Piperidinyl (**3a−c**, **7a−c**) derivatives, **8**, and molecules with a 4-ferrocenyl substituent linked by an ethenyl (**10**, **11**) or ethynyl (**12−14**) spacer have, as their lowest energy transition, band A with $\lambda_{abs}$ > 409 nm ($\epsilon$ > 4000). This is assigned to a CT transition with a singlet excited state representation as shown in Figure 1. There is a complication with the electronic spectrum of molecules with a ferrocenyl headgroup or 4-ferrocenyl substituent in that the ferrocenyl moiety itself has a transition at ∼450 nm. Fortunately, the extinction coefficient for this chromophore is low[15,20] (<500) and the contribution of $\lambda_{abs}$(Fc) and $\epsilon$(Fc) to $\lambda_{abs}$(A) can be ignored; a comparison of $\lambda_{abs}$(A) for the methyl and ferrocenyl headgroup pairs **3c/4** and **7c/9** (Table 2) substantiates this assumption.

The two factors that dominate the shifts in $\lambda_{abs}$(A) are the presence of an unsaturated spacer and, to a lesser extent, the donor capacity of the substituent. The CT

(26) Farrugia, L. J. *J. Appl. Crystallogr.* **1997**, *30*, 565.
(27) Easton, C. J.; Gulbis, J. M.; Hoskins, B. F.; Scharfbillig, I. M.; Tiekink, E. R. T. *Z. Kristallogr.* **1992**, *199*, 249.
(28) (a) Wong, W.-Y.; Lu, G.-L.; Ng, K.-F.; Wong, C.-K.; Choi, K.-H. *J. Organomet. Chem.* **2001**, *637*, 159. (b) Murata, M.; Yamada, M.; Fujita, T.; Kojima, K.; Kurihara, M.; Kubo, K.; Kobayashi, Y.; Nishihara, H. *J. Am. Chem. Soc.* **2001**, *123*, 12903.
(29) (a) Wong-Ng, W.; Nyburg, S. C.; Awwal, A.; Jankie, R.; Kresge, A. J. *Acta Crystallogr.* **1982**, *B38*, 559. (b) Hokelek, T.; Kilic, E.; Tuzun, C. *Acta Crystallogr.* **1991**, *C47*, 369. (c) Sekiguchi, S.; Hosokawa, M.; Suzuki, T.; Sato, M. *J. Chem. Soc., Perkin Trans. 2* **1993**, *6*, 1111. (d) Dijkstra, G. D. H.; *Rec. Trav. Chim. Pays-Bas* **1993**, *112*, 151. (e) Mes, G. F.; Van Ramesdonk, H. J.; Verhoeven, J. W. *J. Am. Chem. Soc.* **1984**, *106*, 1335.
(30) (a) Spek, A. L. *Acta Crystallogr. Sect. A* **1990**, *C34*, 46. (b) Janiak, C. *J. Chem. Soc., Dalton Trans.* **2000**, 3885.

**Table 2. Electrochemical, UV−Vis, and Fluorescence Data**

| | electrochemistry[a] | | UV/vis[c] $\lambda_{abs}$/nm neutral | oxidized[d] | | fluorescence[e] | |
|---|---|---|---|---|---|---|---|
| | $[Fc]^{0/+}$ | $[Naph]^{0/-b}$ | A | CT | $Fc^+$ | $\lambda_{flu}$/nm | $\phi_f$ |
| **3c**[f] | 0.49 | −1.1 | 409 *(11)* | | 630 *(0.2)* | 515 | 0.11 |
| **4** | | | 410 *(10)* | | | 517 | 0.77 |
| **7c**[g] | 0.50 | −1.0 | 491 *(20)* | | 630 *(<0.2)* | 599 | 0.24 |
| **8** | 0.58 | −1.0 | 507 *(22)* | | | 598 | |
| **9** | | | 494 *(19)* | | | 600 | 0.46 |
| **10** | 0.60[h] | −1.0 | 525 *(6)* | 838 *(0.6)* | 625 *(0.5)* | | |
| **11** | 0.60 | −1.0 | 526 *(5)* | 857 *(0.5)* | | | |
| **12** | 0.58 | −1.1 | 505 *(4)* | 788 *(0.8)* | 630 *(0.5)* | | |
| | 0.71 | | | | | | |
| **13** | 0.72 | −1.0 | 506 *(4)* | 800 *(0.7)* | | | |
| **14** | 0.30 | −1.1 | 605 *(4)* | 838 *(0.5)* | | | |

[a] In $CH_2Cl_2$, Pt, 0.1 M $TBAPF_6$, 20 °C. Referenced against decamethylferrocene for which $[Ferrocene]^{+/0} = 0.55$ V. [b] $[Naph]^{0/-}$ irreversible multielectron process. [c] In $CH_2Cl_2$; $\lambda$ nm ($\epsilon$ $mol^{-1}$ $cm^{-1}$ $L \times 10^{-3}$), 20 °C. [d] From OTTLE data, $CH_2Cl_2$, 0.1 M $TBAPF_6$. [e] In $CH_2Cl_2$. [f] $\phi_f$ for **3a**, 0.001; **3b**, 0.02. [g] $\phi_f$ for **7a**, 0.002; **7b**, 0.11. [h] Two-electron process due to superposition of $[FcCH_2]^{+/0}$ and $[FcC{=}C]^{+/0}$

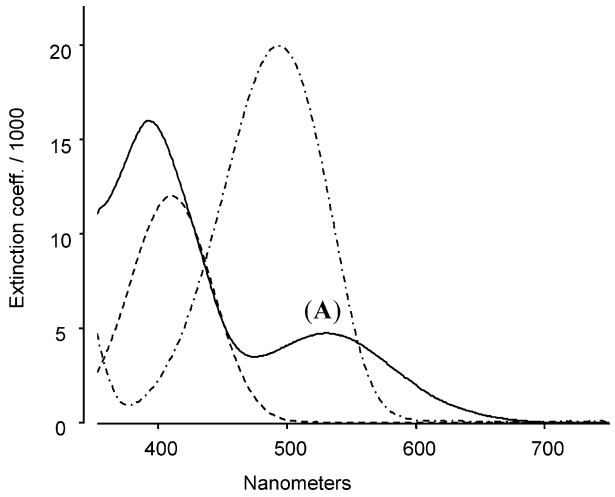


**Figure 4.** Electronic spectra of **3a** (- - -), **7a** (-·-·-·), and **10** (—) in $CH_2Cl_2$. Lowest energy transitions are A.

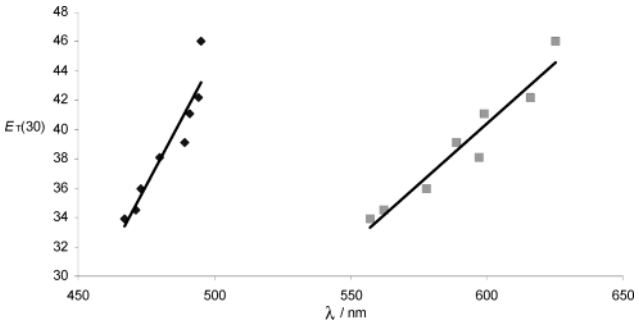


**Figure 5.** Variation of electronic and emission spectra with solvent for **7c**: (♦) $\lambda_{abs}$ vs $E_T(30)$, (■) $\lambda_{flu}$ vs $E_T(30)$.

energies (~24 450 $cm^{-1}$) and peak extinction coefficients (10 000 l $mol^{-1}$ $cm^{-1}$) of band A for derivatives with the piperidine linked directly to the fluorophore **3a**−**c** are similar to those for other 4-aminonaphthalimide compounds.[2,5−7,16] The introduction of a −C≡C− spacer induces a red shift in $\lambda_{abs}$(A) of ~4000 $cm^{-1}$ from **3a**−**c** to **7a**−**c** and an order of magnitude increase in extinction coefficients. There is a further red shift when the enamine is replaced by an ethenylferrocenyl or ethynylferrocenyl donor (cf. **7a** and **10**, **12**) and a concomitant 4-fold drop in extinction coefficient. A significant red shift (3200 $cm^{-1}$) occurs when ferrocenyl is replaced by an octamethylferrocenyl donor (cf. **13** and **14**). In summary, CT energies decrease 4-piperidino ≪ 4-*N*-C≡C− < 4-C≡CFc < 4-C≡C−Fc ≪ 4-C≡CFc[#]. The CT energy for the octamethylferrocenyl derivative **14** is the lowest reported, which indicates that the 4-ferrocenyl substituent has a role in the energy levels for the CT transition. For a specific solvent, the type of headgroup has no influence on $\lambda_{abs}$(A); for example, in $CH_2Cl_2$, $\lambda_{abs}$(A) is 409 ± 1 for **3a**−**c** and 410 nm in **4**. $\lambda_{abs}$(A) displays the classical solvent effect,[2] shifting to lower energy with increased solvent polarity (Figure 5, SI Table 2c).

Fluorescence data for the piperidinyl **3** and **4** and enamine **7**−**9** compounds are given in Table 2 and SI Table 2c. The energy of $\lambda_{flu}$ decreases in order **3a** ≈ **3c** ≈ **4** ≫ **7a** ≈ **7c** ≈ **9**. $\lambda_{flu}$ for the 4-piperidinyl compounds **3a**−**c** are similar to those reported for other 4-aminocompounds with non-ferrocenyl headgroups,[5−9] but those for **7c** and **9** in polar solvents represent the lowest $\lambda_{flu}$ observed. Clearly, the unsaturated spacer is the key factor in determining this sequence; the spacer effect is to decrease the emission energy by a red shift of 85 nm (2750 $cm^{-1}$). Within each series there is minimal effect on $\lambda_{flu}$ with headgroup.

This is not the case with $\phi_f$. For the compounds with only a ferrocenyl headgroup (**3**, **7**, and **8**) significant fluorescence was retained depending on the length of the alkyl chain, vide infra. In those compounds with an additional 4-ferrocenyl substituent (**10**−**14**) almost complete quenching was observed. This decrease in emission is attributed to the usual intramolecular singlet state quenching of the fluorophore by the ferrocenyl redox center.[32] $[Fc]^{+/0}$ at ~0.5 V vs SCE allows for intramolecular electron transfer quenching, although singlet energy transfer from the naphthalimide cannot be ruled out. Approximate free energies of charge separation from donor to acceptor can be derived[14] from $\Delta G_{CS} = E_{ox} - E_{red} - e^2/r_{12}\epsilon - E_s$, where $E_s$, the potential energy of first excited singlet state, is 2.46 eV for ferrocene and $r_{12}$ is the distance between the donor and acceptor. Similarly, the energy of the charge separation state $\Delta E_{CS}$ can be calculated from $\Delta E_{CS} = E_{ox} - E_{red} - e^2/r_{12}\epsilon$. Since the $e^2/\epsilon$ and $E_s$ terms are constant in a given solvent, and $E_{ox} - E_{red}$ is ~1.6 V for $(CH_2)_{11}Fc$ or $(CH_2)_5$-

(31) (a) Pardo, A.; Campanario, J.; Poyato, J. M. L.; Camacho, J. J.; Reyman, D.; Martin, E. *THEOCHEM* **1988**, *43*, 463. (b) Wintgens, V.; Valat, P.; Kossanyi, J.; Biczok, L.; Demeter, A.; Berces, T. *J. Chem. Soc., Faraday Trans.* **1994**, *90*, 411.

(32) Fery-Forgues, S.; Delavaux-Nicot, B. *J. Photochem. Photobiol. A* **2000**, *132*, 137, and references therein.

Fc and ~ 1.7 V for $CH_2Fc$ (these potentials are corrected vs SCE), it follows that $\Delta G_{CS}$ and $E_s$ will be dependent on $1/r_{12}$. Using $1/r_{12}$ from X-ray data gives $\Delta G_{CS}/\Delta E_{CS}$ values of −0.68 eV/1.78 eV for **7a** and −0.58 eV/1.68 eV for **7c**, values that allow for intramolecular electron transfer in these compounds. The solvatochromism normally associated with fluorescence involving a dipolar excited state is clearly seen from the data in Figure 5 (and SI Table 2c). $\lambda_{flu}$ shifts to lower energy, and $\phi_f$ are reduced by an order of magnitude, in polar solvents. Good correlations with solvent parameters [$E_T$(30)][33] are shown in plots against $\lambda_{flu}$ or Stokes shift if the results for methanol are omitted. The values in methanol are generally too high, and there appears to be a specific solvent−solute hydrogen-bonding interaction in the excited state that stabilizes the charge-separated state.[3,4] A plot of $\lambda_{Flu}$ or Stokes shift as a function of the solvent polarity factor $f - 0.5f'$, where $f = (\epsilon - 1)/2\epsilon + 1$ and $f' = (n^2 - 1)/(2n^2 + 1)$, $\epsilon$ is the dielectric constant, and $n$ is the refractive index of the solvent (ignoring the data in methanol), gave excited state dipoles of ~6, ~11, ~9, and ~12 D for **3a**, **3c**, **7a**, and **7c**, respectively. Given the uncertainty in the radius of the ellipsoidal cavity for these compounds, they are within the range of literature values[6,14,16] for aminonaphthalimides and reinforce the view that there is greater charge separation in the excited state when an unsaturated link is involved.

Significant changes occur in both the absorption and emission spectra upon the oxidation of the ferrocenyl unit in the 4-position, but not when the ferrocenyl headgroup is oxidized. Spectra generated using an OTTLE (optically transparent thin layer electrode) cell show that oxidation of **3**−**8** at the [headgroup]$^{+/0}$ potential leaves $\lambda_{abs}$(A) unchanged and a weak feature arises at ~630 nm due to the ferrocenium transition[34] (Figure 6a).

OTTLE spectroscopy of the compounds with a *N*-Me headgroup provided a useful reference in understanding the effect of oxidation of the 4-ferrocenyl substituent. Thus, oxidation of **13** at 0.7 V results in a bleaching of $\lambda_{abs}$(A), and new weak bands arise at 581 and 800 nm (Figure 6b, Table 2). The ~0.2 V difference in the $[FcCH_2]^{+/0}$ and [4-C≡CFc]$^{+/0}$ potentials allowed OTTLE data to be collected for both **12**$^+$ and **12**$^{2+}$ species. The first oxidation process at 0.58 V results in a slight shift of $\lambda_{abs}$(A), masking the 630 nm ferrocenium headgroup absorption. When the potential is increased to 0.71 V, $\lambda_{abs}$(A) is bleached, and bands arise due to the ferrocenium absorption at 630 nm plus the weak bands at 580 and 790 nm as observed for **13**$^+$. The broad transition at 790 nm (12 500 cm$^{-1}$), which has negative solvatochromism, is assigned to a donor−acceptor ($\pi^*$) → C≡CFc$^+$ charge transfer. This type of CT transition has recently been shown to be a characteristic of aromatic-C≡C−Fc$^+$ dyads,[20] where its energy is a function of the donor capacity of the polyaromatic. The relatively high energy of this transition in **13** (for the analogous anthracene dyad the energy is 1200 nm, 8330 cm$^{-1}$) reflects the poor donor capacity of the naphthalimide, and the negative solvatochromism is consistent with a smaller dipole in the excited state. Energies for the ($\pi$) → C=CFc$^+$ CT transition are lower by ~570 cm$^{-1}$ than those for the equivalent fluorophore ($\pi$) → C≡CFc$^+$ transition, a trend found in other aromatic fluorophore systems.[20] OTTLE oxidation of the octamethylethynylferrocene **14** gives results similar to those for **13**, a bleaching of A and generation of a new charge transfer band at 838 nm. As a consequence of the node at the imide N, the headgroup makes little difference to the energies for the CT transition of **12/13** and **10/11** (Table 2).

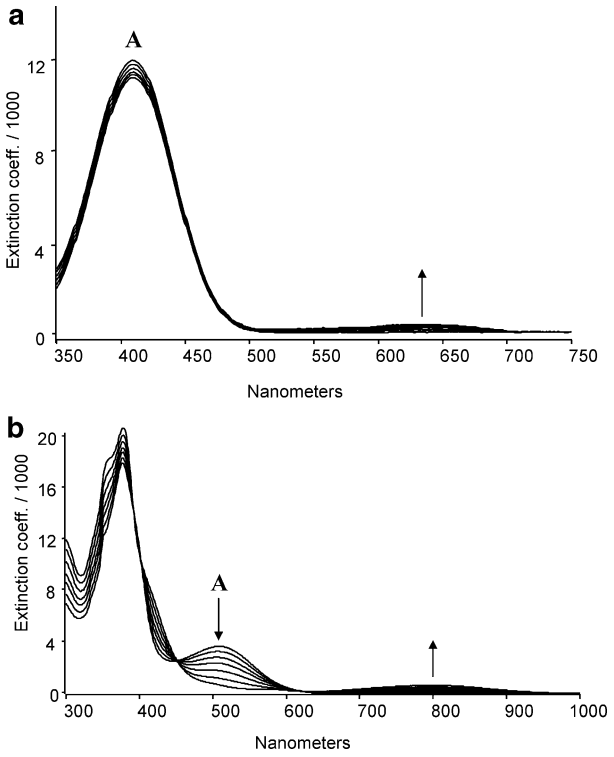


**Figure 6.** (a) OTTLE spectra of **3c**, 0.6 V (1 mM/Pt/$CH_2Cl_2$/0.1 M $TBAPF_6$). (b) OTTLE spectra of **13**, 0.7 V (1 mM/Pt/$CH_2Cl_2$/0.1 M $TBAPF_6$).

The data for **10**−**14** show that upon oxidation to a C=CFc$^+$ or −C≡CFc$^+$ system there is a mixing in of the $\pi$-orbitals of the naphthalimide with the ferrocenyl energy levels, obviating the donor−acceptor charge separation shown in Figure 1. Although this could block the electron transfer quenching mechanism and give dyads with increased emission, both $\lambda_{flu}$ and $\phi_f$ *decreased* upon oxidation. Few results on the effect of oxidation of the ferrocenyl group on $\phi_f$ have been reported,[15,35] but it is clear that either an increase or decrease in $\lambda_{flu}$ is possible. Further work is necessary to elucidate the reason for this dichotomy.

**Radical Anions.** An irreversible reduction couple [$E_p^c$]$^{0/-1}$ (Table 2) due to the formation of the naphthalimide radical anion[36] was observed for all compounds. A study of the radical anions was undertaken, as they could give valuable insight into the LUMO of the neutral molecule. EPR spectra of simple 4-substituted radical anions with amino groups or unsaturated spac-

(33) Reichardt, C. *Angew. Chem., Int. Ed. Engl.* **1979**, *18*, 98.
(34) Sohn, Y. S.; Hendrickson, D. N.; Gray, H. B. *J. Am. Chem. Soc.* **1971**, *93*, 3603.
(35) McGale, E. M.; Robinson, B. H.; Simpson, J. *Organometallics* **2003**, *22*, 931.
(36) Nelsen, S. F.; *J. Am. Chem. Soc.* **1967**, *89*, 5925. Sioda, R. E.; Koski, W. S. *J. Am. Chem. Soc.* **1967**, *89*, 475. Ryabinin, V. A.; Starichenko, V. F.; Vorozhtsov, G. N.; Shein, S. M. *Zhur. Struct. Khim.* **1978**, *19*, 804.

**Table 3. EPR Parameters[a]**

| compd | $g$ | $a^{H}_{2,7}$ | $a^{H}_{3,6}$ | $a^{H}_{4,5}$ | $a^{N}$ | $a^{N}_{amino}$ | $a^{H}_{CHn}$ |
|---|---|---|---|---|---|---|---|
| **1c** | 2.0099 | 4.84 | 0.70 | 5.55 | 1.42 | | 0.70 |
| **2c** | 2.0006 | 4.88 | 0.71 | 5.62 | 1.36 | | |
| **3c** | 2.0033 | 5.28 | 0.38 | 5.28 | 1.46 | 2.68 | |
| **4** | 2.0031 | 5.296 | 0.654 | 7.917 | 1.368 | 7.917 | 0.654 |
| **7a** | 2.0034 | 3.36 | <0.25 | 4.49 (incl =CH) | 2.27 | | 1.13 |
| **9** | 2.0031 | 3.42 (4H) | 0.68 | 4.10 | 1.35 | | |
| **12**[b] | 2.0047 | 0.205 | <0.25 | 1.537 | 0.416 | | 0.416 |
| **13** | 2.0038 | 4.40, 3.21 | <0.25 | 4.40 | 0.61 | | 1.42 |

[a] In $CH_2Cl_2$ at 230 K, generated electrochemically in situ at −1.1 V. [b] HFC to Cp ring 0.23 (4H).

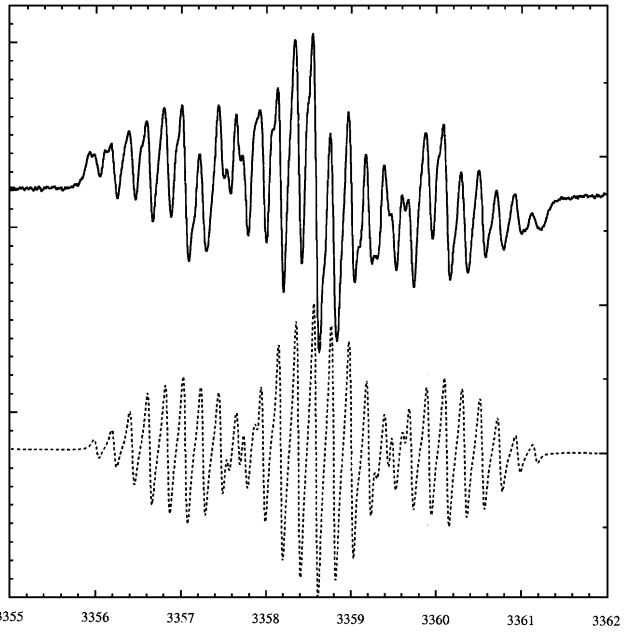


**Figure 7.** EPR of **12**$^{\bullet-}$ in THF/TBAPF$_6$ at 230 K (- - - simulated spectrum).

ers have not been reported, although the electron spin dynamics of a related supramolecular array incorporating a 4-piperazinenaphthalimide unit have been analyzed.[37]

EPR spectra were generated at 250 K and as frozen solutions. Data are given in Table 3 and the EPR spectrum for **12** in Figure 7. Data for a number of other 4-substituted naphthalimide radical anions are also given in Table 3. Hyperfine coupling constants (HFC) and isotropic $g$-values (2.0010−2.0050) for radical anions with a ferrocenyl headgroup are similar to their methyl counterparts. Thus, the presence or absence of a ferrocenyl headgroup has no effect on the unpaired electron distribution in the SOMO of the radical anion or the LUMO of the neutral molecule. Ring HFC for the compounds without an unsaturated spacer **3c** and **4a** are similar to those for **1**$^{\bullet-}$ although there is now significant spin density on the donor nitrogen atom of the piperidine (Table 3). Thus the SOMO is not perturbed by charge separation in the ground state, and this is confirmed by B3LYP calculations. The situation changes when the donor is connected to the $\pi$ system by a delocalized spacer. For **7a**, **9**, **12**, and **13** there is an overall decrease in the spin density on the naphthalimide core, especially $a^{H}_{3,7}$ and $a^{H}_{2,5}$ (Table 3). There is an interesting difference between **7a** and **9** in that HFC reveal a large spin density on the protons of the acyclic piperidine ring with a ferrocenyl, but not methyl headgroup. This is surprising, as the ubiquitous node at the imide should ameliorate any influence of the headgroup, as we have seen in other spectroscopic data. This influence of the headgroup leads to a striking anomaly between **12** and **13**. In **12** the largest proton coupling comes from the four protons on the Cp ring attached to the ethynylferrocene group; the other couplings for **12** are unusually small, whereas those for **13** are similar to those for **9**. This suggests that there is a specific interaction (vide infra) between the two ferrocenyl groups in the ethynyl derivative.

**Influence of Ferrocenyl Headgroups and Unsaturated Spacers on Spectroscopic Properties.** With respect to the 4-substituent the energy of $\lambda_{abs}$(A) decreases in the order 4-C≡CFc[#] ≪ 4-C=C−Fc < 4-C≡CFc. For the amine derivatives **3a**−**c**, **4**, and **7a**−**c**−**9** the energies of both $\lambda_{abs}$(A) and $\lambda_{flu}$ decrease in the order 4-*N*-C=C− ≪ 4-piperidinyl. Fluorescence spectra are mirror images of the charge transfer band, $\lambda_{abs}$(A), indicating that the geometry of the molecule in its relaxed Franck−Condon excited state is not very different from that of the ground state. For a particular 4-substituent the headgroup has a minimal effect on the energies of $\lambda_{abs}$(A) due to the node at the imide.

Clearly, $\pi$-conjugation with the naphthalene core, as depicted in Figure 1, facilitates charge transfer in the singlet excited state, and the unsaturated spacer plays a crucial role. B3LYP calculations were therefore carried out to see if the orbital configurations of the HOMO and LUMO in **7**, **10**, and **12** were different from those in **3**. These calculations revealed that the LUMO is largely associated with the $\pi$-system, but there was a small antibonding component from the −C=C−N and −C=C−Cp moieties, consistent with the EPR results for the SOMO. What was surprising was that the HOMO for molecules with an unsaturated spacer had a configuration with significant electron density on the unsaturated spacer-donor portion of the dyad; the HOMO-1 and lower orbitals had more contribution from the naphthalene core. Configuration interaction leads to a ground state energy level that includes the HOMO and lower HOMO levels, so the ground state, as well as the excited state, has significant contribution from the unsaturated spacer. Once the ferrocenyl headgroup is oxidized, then an additional CT transition is seen which is entirely an excitation involving the unsaturated link and C=CFc$^+$ or C≡CFc$^+$. A consequence of the above results is that the CT energy can be tuned via appropriate donor substitution on the ferrocenyl group. The molecules with the −C=C− and −C≡C− spacer are ideally set up for

(37) Hasharoni, K.; Levanon, H.; Greenfield, S. R.; Gosztola, D. J.; Svec, W. A.; Wasielewski, M. R. *J. Am. Chem. Soc.* **1996**, *118*, 10228.

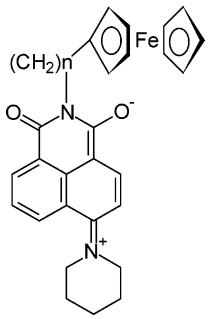


**Figure 8.** Through-space interaction between ferrocenyl headgroup and fluorophore.

facile CT separation, as there is no steric interaction between donor and acceptor; a peri-hydrogen interaction between the ring and amino substituent has been identified in 4-amino compounds.[14] The more effective conjugation of C═CFc compared to C≡CFc has been found also in polyaromatic systems.[20] A ferrocenyl moiety is a good donor, and the magnitude of the difference in CT energy between **7a** and **10** is consistent with the calculations which suggest that the singlet level is strongly perturbed by the ferrocenyl group.

Surprisingly, both the headgroup and spacer have a well-defined influence on quantum yields. $\phi_f$ are >40% higher for molecules with an unsaturated spacer. Furthermore, there is a significant distance effect with $\phi_f$ an order of magnitude greater for $(CH_2)_{11}Fc$ in comparison to a $(CH_2)_5Fc$ headgroup. $\phi_f$ is very small with $CH_2Fc$. $\phi_f$ for the $(CH_2)_{11}Fc$ headgroup molecules were less than half those of *N*-Me analogues. Quenching of the PET process through electron transfer can therefore be tuned by the chain length of the ferrocenyl headgroup. $(CH_2)_{11}Fc$ is the most useful headgroup, as longer chain headgroups tend to form micelles, the properties of which also affect $\phi_f$.[38] This raises the question as to why the nodal effect of the imide, which normally negates any group influence on the spectroscopic properties of 1,8-naphthalimides, is ameliorated for the quantum yield. For the radical anions there was also a significant difference in HFC between alkylferrocenyl and methyl headgroup analogues **12/13**. We suggest that the flexibility of the alkylferrocenyl headgroup is a factor that needs to be considered. Once a charged species is produced, either as radical anion or in the charge-separated excited state, it is possible that the headgroup rotates (Figure 8) so that the ferrocenyl moiety is orientated close to the atom bearing the negative charge (the imide carboxyl group), thereby perturbing the spin density on the radical anion or lifetime of the excited state. Such a through-space interaction would be more efficient in the $(CH_2)$ than $(CH_2)_{11}$ headgroup and would have more of an effect on the lifetime than the excited state energy.

## Conclusion

By an appropriate choice of chain length it is possible to exploit a distance effect and tune dyads with an alkylferrocenyl headgroup to give reasonable emission. The 4-substituted molecules with the unsaturated spacer are ideally set up for facile CT separation; enamine dyads are consequently highly fluorescent. Furthermore, the CT energy can be tuned via appropriate donor substitution on the ferrocenyl group in the 4-position. Once the ferrocenyl termini are oxidized, the dyads show behavior typical of polar headgroup surfactants. In our laboratories, these features have been successfully incorporated into polymers.

## Experimental Section

Solvents were dried and distilled by standard procedures, and all reactions were performed under nitrogen. 4-Bromo-*N*-(alkylferrocenyl)-1,8-naphthalimide (**2a**−**c**),[15] 4-ethynylferrocenyl-*N*-methylferrocenyl-1,8-naphthalimide (**12**),[15] ethenylferrocene,[39] ethynylferrocene,[40] and octamethylethynylferrocene[41] were prepared by published methods. Other commercial reagents (Aldrich) were used as received. Microanalyses were carried out by the Campbell Microanalytical Laboratory, University of Otago. Mass spectra were recorded on a Kratos MS80RFA instrument with an Iontech ZN11NF atom gun. IR spectra were recorded on a Perkin-Elmer Spectrum BX FT-IR spectrometer; $^1H$ and $^{13}C$ NMR spectra on Varian Unity Inova 300 and 500 MHz spectrometers in $CDCl_3$ at 25 °C; electronic and emission spectra were recorded on Varian Cary 500 UV−vis and Perkin-Elmer LS 50B spectrophotometers, respectively. Fluorescence measurements were conducted on optically dilute samples (absorbance <0.05) in spectroscopic grade solvents, and the quantum yield was calculated by comparing the integrated fluorescence spectra with a comparable compound, 4-piperidinyl-*N*-methyl-1,8-naphthalimide (**4**) ($\phi_f$ = 0.91)[21] and Rhodamine 6G (ethanol $\phi_f$ = 0.94). The estimated error in the determination of $\phi_f$ was 20%. Cyclic and square-wave voltammetry in $CH_2Cl_2$ were performed using a three-electrode cell with a polished disk, Pt (2.27 $mm^2$) as the working electrode; solutions were ~$10^{-3}$ M in electroactive material and 0.10 M in supporting electrolyte (triply recrystallized $TBAPF_6$). Data were recorded on a Powerlab/4sp computer-controlled potentiostat. Scan rates of 0.05−1 V $s^{-1}$ were typically employed for cyclic voltammetry and for square-wave voltammetry, square-wave step heights of 5 mV, and a square amplitude of 25 mV with a frequency of 15 Hz. All potentials are referenced to decamethylferrocene; $E_{1/2}$ for sublimed ferrocene was 0.55 V. Infrared and UV−vis OTTLE data were obtained from standard cells with platinum grid electrodes. OTTLE spectra for most compounds had clean isosbestic points, the exception being spectra of **7a**$^+$ due to rapid decomposition of the cation. EPR spectra were obtained using a Bruker EMX X-band spectrometer equipped with a Bruker variable-temperature accessory, a Systron-Donner microwave frequency counter, and a Bruker gaussmeter; ca. 5 mM THF/$TBAPF_6$ solutions of the compound were reduced electrochemically in situ. Ab initio calculations were performed by DFT methods using Gaussian 98 software.[42,43] The basis set was 6-31G(d). Molecular orbital contour plots were prepared by importing the Gaussian 98 output files into MOLDEN.[43] Experimental data for **3b/c** and **5b/c**−**7b/c** are given in the Supporting Information.

**Preparation of 3a.** 4-Bromo-*N*-$CH_2$Fc-1,8-naphthalimide, **2a** (0.118 g, 0.25 mmol), was heated in piperidine (5 mL) for 1.5 h. The solvent was removed in vacuo and the residue purified by column chromatography ($SiO_2/CH_2Cl_2$) to give an

(38) McAdam, C. J. Unpublished work.

(39) Liu, W.-Y.; Xu, Q.-H.; Ma, Y.-X.; Liang, Y.-M.; Dong, N.-L.; Guan, D.-P. *J. Organomet. Chem.* **2001**, *625*, 128.
(40) Abram, T. S.; Watts, W. E. *Synth. React. Inorg. Metal-Org. Chem.* **1976**, *6*, 31.
(41) Jutzi, P.; Kleinebekel, B. *J. Organomet. Chem.* **1997**, *545*−*6*, 573.
(42) *PC SPARTAN Plus* Version 1.5; Wavefunction Inc.: 18401 Von Karman Ave., Suite 370, Irvine, CA 92612, 1998.
(43) Schaftenaar, G.; Noordik, J. H. *J. Comput.-Aided Mol. Des.* **2000**, *14*, 123.

orange band, from which orange crystals of **3a** were obtained on removal of the solvent, 0.115 g (96%). Anal. Calcd for $C_{28}H_{26}FeN_2O_2$: C, 70.30; H, 5.48; N, 5.86. Found: C, 70.17; H, 5.60; N, 5.95. EI-MS: *m/e* 478 ($M^+$). $^1$H NMR: $\delta$ 1.70 (m, 2H, pip.-H), 1.87, 3.20 {2 × (m, 4H, pip.-H)}, 4.06, 4.50 {2 × (t, 2H, Fc-H)}, 4.21 (s, 5H, $-C_5H_5$), 5.11 (s, 2H, $-CH_2$-Fc), 7.14 {d ($J$ = 8.1 Hz), naphth H3}, 7.64 {dd ($J$ = 8.5, 7.3 Hz), naphth H6}, 8.35 {dd ($J$ = 8.5, 1.2 Hz), naphth H5}, 8.47 {d ($J$ = 8.1 Hz), naphth H2}, 8.54 {dd ($J$ = 7.3, 1.2 Hz), naphth H7}. IR (KBr, $cm^{-1}$): $\nu_{C=O}$ 1694, 1656.

**Preparation of 5a. 2a** (0.324 g, 0.68 mmol) and trimethylsilylacetylene (0.134 g, 1.37 mmol) were added to 50 mL of degassed diisopropylamine containing 2% CuI and 2% $PdCl_2(PPh_3)_2$. The resulting cloudy gray suspension was heated to reflux for 2 h. Solvent was removed in vacuo, and the yellow powder obtained was purified by column chromatography ($SiO_2/CH_2Cl_2$). The first band eluted yielded a pale yellow solid **5a**, 0.3 g (89%). Anal. Calcd for $C_{28}H_{25}FeNO_2Si$: C, 68.43; H, 5.13; N, 2.85. Found: C, 68.43; H, 5.35; N, 2.94. EI-MS: *m/e* 491 $(M)^+$. $^1$H NMR: $\delta$ 0.35 (s, 9H, Si-C*H*$_3$), 4.08, 4.50 {2 × (t, 2H, Fc-*H*)}, 4.21 (s, 5H, $-C_5H_5$), 5.12 (s, 2H, $-CH_2$-Fc), 7.79 {dd ($J$ = 8, 7.5 Hz), naphth *H*6}, 7.87 {d ($J$ = 8 Hz), naphth *H*3}, 8.49{d ($J$ = 8 Hz), naphth *H*2}, 8.59 (m, 2H, naphth *H*5 and 7). IR (KBr, $cm^{-1}$): $\nu_{C\equiv C}$ 2152, $\nu_{C=O}$ 1699, 1662.

**Preparation of 6a. 5a** (0.16 g, 0.33 mmol) and $K_2CO_3$ (0.18 g, 1.3 mmol) were stirred in 50 mL of methanol at room temperature for 2 h. The solvent was removed under vacuum, and then the product dissolved in $CH_2Cl_2$ and filtered. Precipitation with $CH_2Cl_2$/hexane yielded **6a** as an orange-yellow powder (0.124 g, 91%). Anal. Calcd for $C_{30}H_{28}FeNO_2$: C, 71.62; H, 4.09; N, 3.34. Found: C, 71.30; H, 4.42; N, 3.41. EI-MS: *m/e* 419 $(M)^+$. $^1$H NMR: $\delta$ 3.69 (s, 1H, C≡C*H*), 4.09, 4.51 {2 × (t, 2H, Fc-*H*)}, 4.21 (s, 5H, $-C_5H_5$), 5.12 (s, 2H, $-CH_2$-Fc), 7.74 {dd ($J$ = 8.1, 7.2 Hz), naphth *H*6}, 7.84 {d ($J$ = 7.5 Hz), naphth *H*3}, 8.46 {d ($J$ = 7.5 Hz), naphth *H*2}, 8.55 {dd ($J$ = 8.1, 1.2 Hz), naphth *H*5}, 8.56 {dd ($J$ = 7.2, 1.2 Hz), naphth *H*7}. IR (KBr, $cm^{-1}$): $\nu_{C\equiv C}$ 2098, $\nu_{C=O}$ 1697, 1652.

**Preparation of 7a. 6a** (0.05 g, 0.21 mmol) was stirred in piperidine (20 mL). The reaction mixture changed from a pale yellow color to red almost instantaneously. After stirring for 16 h the piperidine was removed under reduced pressure. The resulting dark red solid was dissolved in $CH_2Cl_2$, washed with water (4 × 20 mL) to remove any residual piperidine, and dried ($MgSO_4$), and the solvent was removed under vacuum. Recrystallization of the red solid from $CH_2Cl_2$ layered with hexane yielded **7a** as a dark red solid (0.048 g, 71%). Anal. Calcd for $C_{30}H_{28}FeN_2O_2 \cdot 1/2H_2O$: C, 70.18; H, 5.85; N, 5.46. Found: C, 70.09; H, 5.69; N, 5.54. EI-MS: *m/e* 504 $(M)^+$. $^1$H NMR: $\delta$ 1.68 (m, 6H, piperidine-*H*), 3.30 (m, 4H, piperidine-*H*), 4.05, 4.51 {2 × (t, 2H, Fc-*H*)}, 4.20 (s, 5H, $-C_5H_5$), 5.11 (s, 2H, $-CH_2$-Fc), 5.99 {d ($J$ = 13 Hz), 1H, C=C*H*-naphth}, 7.09 {d ($J$ = 13 Hz), 1H, C=C*H*-pip}, 7.55 {d ($J$ = 8.4 Hz), naphth *H*3}, 7.60 {dd ($J$ = 8.7, 7.2 Hz), naphth *H*6}, 8.38 {d ($J$ = 8.4 Hz), naphth *H*2}, 8.42 {dd ($J$ = 8.7, 1 Hz), naphth *H*5}, 8.54 {dd ($J$ = 7.2, 1 Hz), naphth *H*7}. IR (KBr disk): $\nu_{C=O}$ 1685, 1651.

**Preparation of 8. 8** was obtained from **6a** as a dark red-purple powder by a procedure similar to that for **7a** (53%) using pyrrolidine as solvent. Anal. Calcd for $C_{29}H_{26}FeN_2O_2 \cdot H_2O$: C, 68.50; H, 5.51; N, 5.51. Found: C, 68.83; H, 5.48; N, 5.85. EI-MS: *m/e* 490 $(M)^+$. $^1$H NMR: $\delta$ 2.01 (m, 4H, pyrrolidine-*H*), 3.44 (m, 4H, pyrrolidine-*H*), 4.05, 4.51 {2 × (t, 2H, Fc-*H*)}, 4.20 (s, 5H, $-C_5H_5$), 5.11 (s, 2H, $-CH_2$-Fc), 5.75 {d ($J$ = 13 Hz), 1H, C=C*H*-pyrr}, 7.48 {d ($J$ = 13 Hz), 1H, C=C*H*-naphth}, 7.53 {d ($J$ = 8.1 Hz), naphth *H*3}, 7.57 {dd ($J$ = 8.7, 7.2 Hz), naphth *H*6}, 8.34 {d ($J$ = 8.1 Hz), naphth *H*2}, 8.41 {dd ($J$ = 8.7, 1 Hz), naphth *H*5}, 8.53 {dd ($J$ = 7.2, 1 Hz), naphth *H*7}. IR (KBr disk, $cm^{-1}$): $\nu_{C=O}$ 1684, 1645.

**Preparation of 10 and 11.** Ethenylferrocene (0.212 g, 1 mmol), **2a** (0.332 g, 0.7 mmol), tri-*o*-tolylphosphine (0.03 g, 0.1 mmol), Pd(II) acetate (0.095 g, 0.4 mmol), and $NEt_3$ (0.6 mL) were heated at 80 °C in 30 mL of DMF for 16 h. Solvent was removed under vacuum, and the reaction mixture was extracted into $CH_2Cl_2$ and then separated using chromatography on $SiO_2$ with a $CH_2Cl_2$ eluant to give dark red crystals of **10** (0.352 g, 83%). Anal. Calcd for $C_{35}H_{27}Fe_2NO_2$: C, 69.45; H, 4.50; N, 2.31. Found: C, 69.27; H, 4.39; N, 2.21. ES-MS: 605 $(M^+)$. $^1$H NMR ($CDCl_3$): $\delta$ 4.09, 4.52 {2 × (t, 2H, Fc-*H*)}, 4.21 (s, 5H, $C_5H_5$, ethenyl Fc), 4.22 (s, 5H, $-C_5H_5$), 4.42 (t, 2H, Fc-$H_\beta$, ethenyl Fc), 4.60 (t, 2H, Fc-$H_\alpha$, ethenyl Fc), 5.14 (s, 2H, $-CH_2-$), 7.18 [d ($J$ = 16 Hz), Fc-C*H*=], 7.46 [d ($J$ = 16 Hz), =C*H*-naphth], 7.75 [dd ($J$ = 8.5, 7.2 Hz), naphth *H*6], 7.92 [d ($J$ = 7.7 Hz), naphth *H*3], 8.50 [dd ($J$ = 8.5, 1.0 Hz), naphth *H*5], 8.55 [d ($J$ = 7.7 Hz), naphth *H*2], 8.61 [dd ($J$ = 7.2, 1.0 Hz), naphth *H*7]. IR (KBr, $cm^{-1}$): $\nu_{C=O}$ 1694, 1656, $\nu_{E-CH=CH\ wag}$ 950.

**11** was obtained as red crystals by a similar procedure from ethenylferrocene and 4-bromo-*N*-Me-naphthalimide (58%). Anal. Calcd for $C_{25}H_{19}FeNO_2$: C, 71.28; H, 4.55; N, 3.33. Found: C, 71.35; H, 4.82; N, 3.29. ES-MS: 422 $(M^+)$. $^1$H NMR ($CDCl_3$): $\delta$ 3.56 (s, 3H, *N-Me*), 4.21 (s, 5H, $C_5H_5$), 4.27 (t, 2H, Fc-$H_\beta$), 4.60 (t, 2H, Fc-$H_\alpha$), 7.19 [d ($J$ = 16 Hz), Fc-C*H*=], 7.46 [d ($J$ = 16 Hz), =C*H*-naphth], 7.76 [dd ($J$ = 8.5, 7.2 Hz), naphth *H*6], 7.93 [d ($J$ = 7.7 Hz), naphth *H*3], 8.55 [d ($J$ = 7.7 Hz), naphth *H*2], 8.51 [dd ($J$ = 8.5, 1.0 Hz), naphth *H*5], 8.61 [dd ($J$ = 7.2, 1.0 Hz), naphth *H*7]. IR (KBr, $cm^{-1}$): $\nu_{C=O}$ 1700, 1655, $\nu_{E-CH=CH\ wag}$ 950.

**Preparation of 13 and 14.** Ethynylferrocene (0.120 g, 0.57 mmol), 4-bromo-*N*-Me-naphthalimide (0.128 g, 0.44 mmol), and catalytic amounts (0.2 mol %) of $PdCl_2(PPh_3)_2$ and CuI were heated at 75 °C in 10 mL of $^iPr_2NH$ for 30 min. Solvent was removed under vacuum and the reaction mixture separated using chromatography on $SiO_2$ with a $CH_2Cl_2$ eluant to give dark red crystals of **13** (0.166 g, 90%). Anal. Calcd for $C_{25}H_{17}FeNO_2$: C, 71.62; H, 4.09; N, 3.34. Found: C, 71.21; H, 4.37; N, 3.28. ES-MS: 420 $(MH^+)$. $^1$H NMR ($CDCl_3$): $\delta$ 3.57 (s, 3H, *N-Me*), 4.31 (s, 5H, $C_5H_5$), 4.39 (t, 2H, Fc-$H_\beta$), 4.66 (t, 2H, Fc-$H_\alpha$), 7.84 [dd ($J$ = 8.3, 7.3 Hz), naphth *H*6], 7.89 [d ($J$ = 7.6 Hz), naphth *H*3], 8.54 [d ($J$ = 7.6 Hz), naphth *H*2], 8.65 [dd ($J$ = 7.3, 1.1 Hz), naphth *H*7], 8.69 [dd ($J$ = 8.3, 1.1 Hz), naphth *H*5]. IR (KBr, $cm^{-1}$): $\nu_{C\equiv C}$ 2200, $\nu_{C=O}$ 1697, 1658.

**14** was obtained as dark green crystals by a similar procedure from 4-bromo-*N*-Me-naphthalimide and octamethylethynyl ferrocene (74%). Anal. Calcd for $C_{33}H_{33}FeNO_2$: C, 74.58; H, 6.26; N, 2.64. Found: C, 74.31; H, 6.55; N, 2.34. ES-

**Table 4. Crystal Data and Structure Refinement for 3a and 12**

| | 3a | 12 |
|---|---|---|
| empirical formula | $C_{28}H_{26}N_2O_2Fe$ | $C_{35}H_{25}NO_2Fe_2$ |
| fw | 478.36 | 603.26 |
| cryst syst | triclinic | triclinic |
| space group | $P\bar{1}$ | $P\bar{1}$ |
| abs coeff, $mm^{-1}$ | 0.726 | 1.188 |
| final $R$ indices $[I > 2\sigma(I)]$ | R1 = 0.0271 | R1 = 0.0313 |
| | wR2 = 0.0711 | wR2 = 0.0826 |
| $R$ indices (all data) | R1 = 0.0312 | R1 = 0.0422 |
| | wR2 = 0.0730 | wR2 = 0.0852 |
| goodness-of-fit on $F^2$ | 1.041 | 1.053 |
| temp, K | 163(2) | 163(2) |
| wavelength, Å | 0.71073 | 0.71073 |
| $a$, Å | 7.654(2) | 11.352(3) |
| $b$, Å | 10.030(3) | 11.451(3) |
| $c$, Å | 14.447(4) | 12.164(3) |
| α, deg | 101.584(4) | 73.045(3) |
| $\beta$, deg | 94.022(4) | 65.042(3) |
| $\gamma$, deg | 91.813(4) | 62.258(3) |
| $V$, Å$^3$ | 1082.6(6) | 1259.8(6) |
| $Z$ | 2 | 2 |
| density(calcd), $Mg/m^3$ | 1.467 | 1.590 |
| no. of reflns collected | 14096 | 16514 |
| no. of indep reflns | 4374 ($R$(int) = 0.0209) | 5133 ($R$(int) = 0.0252) |

MS: 531 ($M^+$). $^1$H NMR ($CDCl_3$): $\delta$ 3.58 (s, 3H, *N-Me*), 1.71, 1.76, 1.86, 2.05 {4 × (s, 6H, Fc-C$H_3$)}, 3.39 (s, 1H, Fc-*H*), 7.82 [dd ($J$ = 8.4, 7.3 Hz), naphth *H*6], 7.89 [d ($J$ = 7.8 Hz), naphth *H*3], 8.54 [d ($J$ = 7.8 Hz), naphth *H*2], 8.65 [dd ($J$ = 7.3, 1.2 Hz), naphth *H*7], 8.74 [dd ($J$ = 8.4, 1.2 Hz), naphth *H*5]. IR (KBr, $cm^{-1}$): $\nu_{C\equiv C}$ 2188; $\nu_{C=O}$ 1692, 1656.

**X-ray Data Collection, Reduction and Structure Solution for 3a and 12.** Crystal data for **3a** and **12** are given in Table 4. Recrystallization of **12** from $CH_2Cl_2$/hexane yielded dark red plates, and that of **3a** from $CH_2Cl_2$ yielded orange plates. These were used for data collection. Data were collected for both crystals at 168(2) K on a Bruker Smart CCD diffractometer, processed using SAINT,[44] with empirical absorption corrections applied using SADABS.[45] The structure of **3a** was solved by direct methods and **12** by Patterson methods using SHELXS.[46] The structures were refined by full-matrix least-squares using SHELXL-97[46] and TITAN2000.[47] Non-hydrogen atoms were assigned anisotropic temperature factors, and H atoms were included in calculated positions using a riding model for both molecules.

**Acknowledgment.** We thank the University of Otago and the Marsden Fund, Royal Society of NZ, for financial support, Prof. W. T. Robinson (University of Canterbury) for X-ray data collection, and Dr. K. C. Gordon for helpful discussions.

**Supporting Information Available:** A listing of crystal data and structure refinement, atomic coordinates, anisotropic displacement parameters, bond lengths and angles for **3a** and **12**, additional spectroscopic and experimental data, and a scheme showing hydrolysis of the enamine compounds.

OM0304659

(44) *SMART CCD software*; Bruker AXS: Madison WI, 1994.
(45) *SADABS* (correction for area detector data); Bruker AXS: Madison WI, 1997.
(46) Sheldrick, G. M. *SHELXS*, A program for the solution of crystal structures from diffraction data; University of Göttingen: Germany, 1990. Sheldrick, G. M. *SHELXL-97*, A program for the refinement of crystal structures; University of Göttingen: Germany, 1997.
(47) Hunter, K. A.; Simpson, J. *TITAN2000*, A molecular graphics program to aid structure solution and refinement with the SHELX suite of programs; University of Otago: New Zealand, 1999.